Resonant Charge Transfer of Hydrogen Rydberg Atoms Incident on a Cu(100) Projected Band-Gap Surface

J. A. Gibbard, M. Dethlefsen, M. Kohlhoff, C. J. Rennick, E. So, M. Ford, and T. P. Softley
Department of Chemistry, University of Oxford, Chemistry Research Laboratory, Oxford OX1 3TA, United Kingdom
(Received 5 May 2015; revised manuscript received 5 July 2015; published 28 August 2015)

The charge transfer (ionization) of hydrogen Rydberg atoms ($n = 25$–34) incident on a Cu(100) surface is investigated. Unlike fully metallic surfaces, where the Rydberg electron energy is degenerate with the conduction band of the metal, the Cu(100) surface has a projected band gap at these energies, and only discrete image states are available through which charge transfer can take place. Resonant enhancement of charge transfer is observed for Rydberg states whose energy matches one of the image states, and the integrated surface ionization signals (signal versus applied field) show clear periodicity as a function of n as the energies come in and out of resonance with the image states. The surface ionization dynamics show a velocity dependence; decreased velocity of the incident H atom leads to a greater mean distance of ionization and a lower field required to extract the ion. The surface ionization profiles for "on resonance" n values show a changing shape as the velocity is changed, reflecting the finite field range over which resonance occurs.

DOI: 10.1103/PhysRevLett.115.093201 PACS numbers: 34.35.+a, 32.80.Ee, 34.50.Fa, 34.70.+e

The collision of a Rydberg atom with a solid surface typically leads to the transfer of the Rydberg electron to the surface at distances less than $5n^2a_0$, where n is the Rydberg principal quantum number. This is especially true for metallic surfaces, where the Rydberg energy is degenerate with the conduction band so that resonant charge transfer (RCT) occurs. Experimental and theoretical studies of this phenomenon have focused on the effects of varying n, the parabolic quantum number k, the velocity of the incoming particle and the applied fields [1,2], and observing how the ionization rate varies with distance from the surface [3]. For nonhydrogenic atoms, adiabatic and nonadiabatic passage through surface-induced energy level crossings leads to behavior that varies with the Rydberg species [4]. Thus, such studies reveal important information about the Rydberg states and their dynamics near surfaces. An equally important question addresses what such studies reveal about the nature of the surface. Experimental studies have been primarily conducted with flat-metal surfaces for which the ionization dynamics are almost independent of the material because of the generic behavior of RCT to the conduction band. However, there have also been experimental and/or theoretical investigations of the effects of adlayers and thin insulating films [5], interaction with doped semiconductors [6] and dielectric materials [7], and the effects of corrugation and patch charges [8,9]. Related theoretical calculations investigated the variation of ionization rate of ground state H^- with the thickness of a metal film substrate [10]. All of these studies point to a degree of sensitivity of the charge transfer process to the surface characteristics. The mean radius of a hydrogenic Rydberg orbit is of order n^2a_0 (e.g., ~20 nm for $n = 20$) and charge transfer typically occurs at a Rydberg-surface distance of 3–$5n^2a_0$. Thus, information revealed about the *geometrical* structure of the surface is limited to nanoscale features.

In this Letter we investigate the RCT of hydrogen Rydberg atoms ($n = 25$–34) incident on a Cu(100) surface and probe the role of surface *electronic* structure through the resonant nature of the process. Cu(100) has a band gap at the energy of the Rydberg states and RCT can only occur via "image-charge states." An electron outside the surface at a distance z gives rise to an image-charge attractive potential given by (for a perfect conductor) $V(z) = -(1/4z)$. This one-dimensional Coulomb-like potential can support an infinite series of bound states forming a Rydberg-type series with energies given by

$$E_{\mathrm{IS}}(n_{\mathrm{img}}) = -\frac{1}{16}\,\frac{1}{2(n_{\mathrm{img}}+a)^2}, \tag{1}$$

where n_{img} is the image-state index and a the quantum defect parameter for a given surface. For Cu(111) $a \approx 0.02$ and for Cu(100) $a \approx 0.24$ [11]. Such states are only observable in the band-gap range, as those degenerate with the conduction band are mixed and broadened into the band. In the direction parallel to the surface (for both surface and image states), the wave function is very similar to the bulk metal states and energy is not quantized. In the nearly free-electron model, the states form bands with energy

$$\epsilon(k) = E_{\mathrm{IS}} + \frac{\hbar^2}{2m}(k_x^2 + k_y^2), \tag{2}$$

where E_{IS} is the energy of the state with zero parallel momentum [Eq. (1)]. There may also be intrinsic surface

states in the band gap; whereas for image states the wave function is almost entirely outside the metal, for surface states it is located at the surface with some significant penetration inside (cf. valence and Rydberg states of isolated molecules). Surface and image-charge states have been studied experimentally for various materials using time-resolved two-photon photoemission, inverse photoemission, and scanning tunneling spectroscopy [12–14].

The current Letter extends earlier studies of charge transfer between ground-state cesium atoms or H^- and a Cu(111) surface [15,16], and studies of reverse charge transfer to H or Li^+ from a Cu(111) surface [17]. In a recent work we used a wave packet propagation method to calculate surface ionization rates versus distance for a moving Rydberg H atom ($n = 2$–8) incident at Cu(111) and Cu(100) surfaces [18]. We predicted that, for both surfaces, resonances between the energy of the surface-localized image states and the Rydberg atom result in enhancement of the surface ionization process [18] leading to charge transfer at greater distance from the surface. However the low-n states considered there are not usable experimentally due to their short lifetimes for radiative decay. Here, we use the long-lived $n = 25$–34 states, which fall within the band gap of the Cu(100) surface.

Figure 1 shows the predicted energies of the $n = 25$–34 $k = 0$ H atom states and the surface-localized image states as a function of applied field. k runs from $-(n - |m_l| - 1)$ and $(n - |m_l| - 1)$, but only the mid-Stark-manifold $k = 0$ Rydberg states are studied; their energies are approximately field independent and are also the least perturbed by the surface, as indicated by the narrow widths of the blue lines in Fig. 1. The $k = 0$ states provide the greatest range of field for crossing with the field-dependent image-state

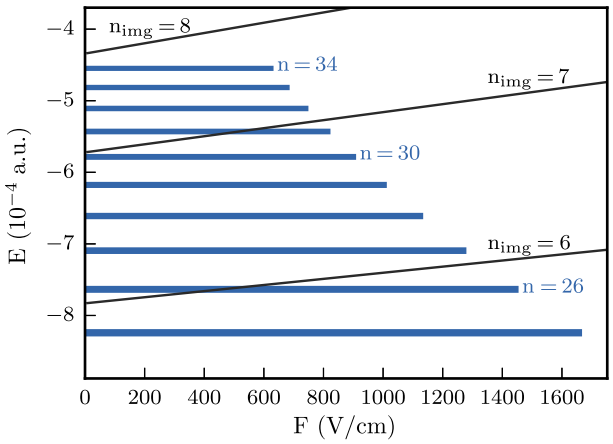

FIG. 1 (color online). The energies of the $n = 25$–36 $k = 0$ H atom states, and the image states ($n_{img} = 6$ to $n_{img} = 8$) of the Cu(100) surface. The widths of the H atom lines represent the range of surface perturbation of the $k = 0$ states for distances from the surface of $3n^2a_0$ to $6n^2a_0$. The lengths of the lines indicate the range of applied fields over which surface ionization can be measured, before the onset of field ionization.

energies, at which resonance-enhanced charge transfer is expected.

The image-state and Rydberg atom energies are calculated independently by diagonalization of a Hamiltonian using a discrete variable representation (DVR) basis set [19]. In the first case the Hamiltonian is appropriate for an electron interacting with its own image charge in a Cu(100) surface, while in the second case it describes a Rydberg atom outside a jellium surface. It was not possible to calculate both sets of energies by diagonalization of the same Hamiltonian as a very large basis set would be required for convergence. A significant approximation is the omission of the ion core of the Rydberg atom when calculating the image-charge states.

The experimental setup to measure the H atom-surface interactions was described previously [1]. In brief, H atoms are formed by photolysis of a supersonic beam of NH_3 at 193 nm in a capillary mounted on the pulsed nozzle [20]. Using a pure NH_3 beam, the H atoms travel 50 cm to the laser excitation point where the high-n (25–34) Rydberg states are populated by two-color ($\lambda_1 = 121.57$ nm, $\lambda_2 = 365.75$–366.75 nm), two-photon excitation via the $2p$ intermediate level. Excitation occurs in a large enough field to allow selection of a specific Stark state (here $k = 0$) of the n manifold. The radiative lifetime of the $n = 30$ H atom Rydberg state in the presence of an applied electric field is > 100 μm [21]. As shown in Fig. 2(a), the Rydberg

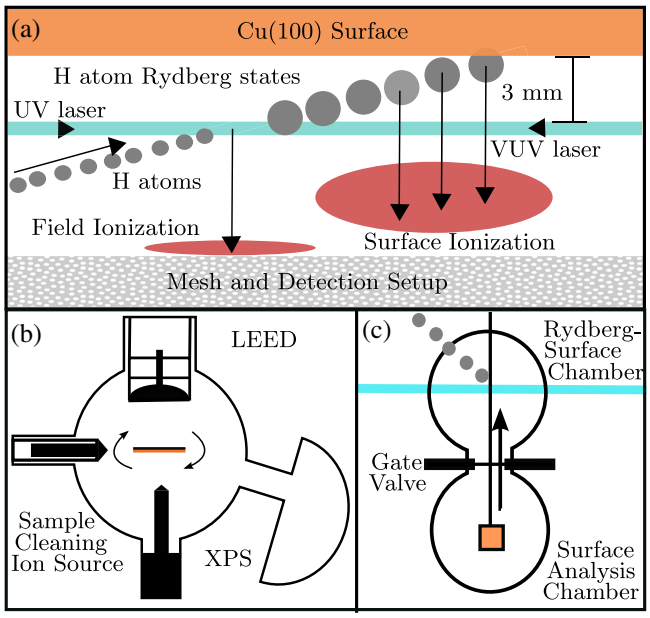

FIG. 2 (color online). (a) Two-color excitation of H atoms produces a beam of Rydberg atoms to probe a Cu(100) surface. Field and surface ionization signals are spatially and temporally separated due to the different ionization positions with respect to the surface. (b) Schematic of the surface analysis chamber. (c) The xyz manipulator allows the surface to be moved between the surface analysis chamber and the Rydberg-surface experiment under vacuum.

atoms then travel 3 mm for ~5 μm to interact with the surface, which is mounted at a 15° incidence angle with respect to the atom beam. The surface can be moved under vacuum to a surface analysis chamber [Fig. 2(b)] where low energy electron diffraction (LEED) and x-ray photoelectron spectroscopy (XPS) are used to determine the elemental composition, crystal plane, and presence of impurities on the surface. The single crystal Cu(100) surface (Mateck GmbH) was prepared in vacuum using 30 min of argon-ion bombardment at 500 eV followed by heating at 700 °C for 20 min. Twenty sputtering and annealing cycles produced a clear LEED pattern with the expected fourfold symmetry, and XPS showed only trace oxygen impurities on the surface. This indicated a clean and flat Cu(100) surface.

Ions, resulting from the Rydberg-to-surface electron transfer, are extracted away from the surface to a detector by applying a field perpendicular to the surface. The field is present at the time of ionization and is switched from the initial Stark field 1 μs after excitation. The minimum field required to extract the ions ($\vec{F}_{\rm min}$) depends on the Rydberg-surface separation (D) at which ionization occurs and on the kinetic energy of the incident H atom along the surface normal ($T_\perp$); for a flat, perfectly conducting surface,

$$\vec{F}_{\rm min}(D, T_\perp) = \left[\frac{1}{2D} + \sqrt{\frac{T_\perp}{D}}\right]^2. \quad (3)$$

The mean value of D for a given Rydberg state is mildly dependent on the applied extraction field [2].

Experimentally we observe "surface ionization profiles" as in Fig. 3, each recording the intensity of surface ionization signal (ions) as a function of extraction field. The profiles shift to higher field as n decreases, because ionization occurs closer to the surface and a greater field is required to prevent the ion from being pulled into the surface by its own image charge and velocity. The gradual rise of the signal as the field increases reflects the range of distances over which ionization takes place, but also the surface-charge distribution (patch fields) that affects primarily the extraction probability [9,22]. At sufficiently large fields the Rydberg atom is field ionized before reaching the surface, leading to a high-field cutoff in the surface ionization profile. Ions from direct field ionization are separated in time from the surface ionization signal: the field ionization signal is used to normalize the surface ionization profiles, to account for fluctuations in laser power and molecular beam density.

As discussed below, measuring surface ionization profiles for different velocities provides an extra handle on resonant charge transfer effects. Experimentally, the velocity is varied by changing the delay between the photodissociation laser pulse and the two excitation lasers. Over the 50 cm distance between the photolysis of NH_3 and the Rydberg excitation of H atoms, the atoms spread out in the longitudinal direction according to their velocity; hence, changing the delay picks out a different velocity. For a flat surface, only the perpendicular component is physically significant and, for the H atom beam here, is variable from 500–850 m s^{-1} with a 1% velocity resolution.

Examples of surface ionization profiles are shown in Fig. 3 for three different n values and four different incident velocities, while Fig. 4 plots the integral of the surface ionization profile for $n = 25$–34. The profiles in Fig. 3 appear similar to those measured for H atoms incident at a gold surface [1] (for which RCT can occur at all n values, as there is no band gap). For Cu(100), however, there are larger variations in the intensity of the surface ionization signal as a function of n. The maximum surface ionization

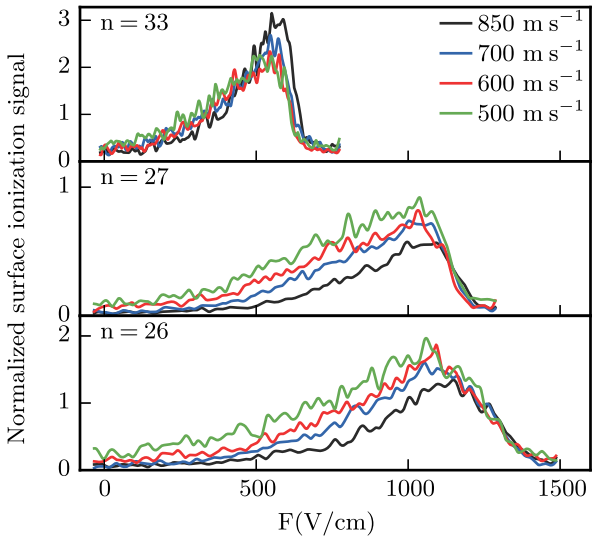

FIG. 3 (color online). H atom surface ionization profiles for $n = 26$, 27, 33 at various perpendicular velocities: black lines, 850 m s^{-1}; red lines, 700 m s^{-1}; green lines, 600 m s^{-1}; blue lines, 500 m s^{-1}.

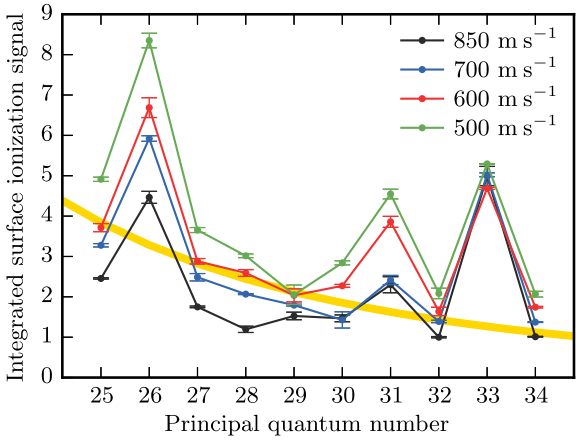

FIG. 4 (color online). The integrated surface ionization signal for H atoms incident on a Cu(100) surface as a function of n. The yellow line shows the corresponding behavior for a gold surface at a velocity of 660 m s^{-1}.

signal (normalized to field ionization) for $n = 26$ is twice that of $n = 27$ (Fig. 3), and the low-field part of the profile is also raised in intensity. Other such higher intensity profiles are seen at $n = 31$ and $n = 33$. The increased intensity at lower extraction fields implies a higher propensity for ionization at a greater distance from the surface.

Figure 4 shows that the integrated surface profile for gold (the yellow line) decreases monotonically as n increases, because the field range over which ions are extracted and over which the signal is integrated decreases with increasing n. For Cu(100), however, clear peaks can be seen at $n = 26, 31$, and 33. We attribute this nonmonotonic behavior to the predicted resonance effect resulting from energy matching between the Rydberg states and the image-charge states. Theoretical calculations for ionization of low-n H atoms at Cu(100) and Cu(111) surfaces [18] show that in the nonresonant case the charge transfer can only occur if the electron takes up significant momentum parallel to the surface. Conservation of angular momentum inhibits the development of parallel momentum (this is a high angular momentum state with respect to the atom), and there is a marked preference for the electron flux to occur perpendicular to the surface. The saddle point in the electronic potential occurs along the perpendicular direction, and hence classically electron transfer should occur in this direction. The calculations predict that resonance enhancement of charge transfer manifests as a shift in surface ionization to larger Rydberg-surface separations, such that there will be more of a surface ionization signal at lower fields, and an overall increase in intensity of the surface ionization profile.

The wave packet calculations cannot be performed currently for $n = 25$–34 because the DVR grid required is unmanageably large for converging calculations. But similar resonant behavior is expected at higher n, as is indeed demonstrated experimentally in Fig. 4. Three image states, $n_{\mathrm{img}} = 6$ to 8, are predicted in Fig. 1 to cross the Rydberg energies at $n = 26, 31$, and 35, respectively, compared to the experimental peaks at $n = 26, 31$, and 33. The approximations in the calculations of Fig. 1, particularly the absence of the ion in the image-state calculation, mean that discrepancies in where resonances occur may be expected, particularly at higher n_{img}; the presence of the ion would tend to pull down the higher image-state energies.

Each connected set of points in Fig. 4 represents the integrated surface signal for different incident velocities of hydrogen. In general, the variations with velocity are greater for the resonant n values than for the off-resonant values. For resonant n, the signal enhancement occurring as the velocity is lowered tends to lead to a change in shape of the profile. For example, for $n = 33$ the 850 $\mathrm{m\,s^{-1}}$ signal (Fig. 3, the black line) lies above the 850 $\mathrm{m\,s^{-1}}$ signal (the green line) at 550 $\mathrm{V\,cm^{-1}}$, but below it at 300 $\mathrm{V\,cm^{-1}}$. For the off-resonant n, the signal amplitude simply scales up as the velocity decreases, and the signal increase is greater at lower-field values—e.g., for $n = 27$ the signal at 500 $\mathrm{V\,cm^{-1}}$ and velocity 500 $\mathrm{m\,s^{-1}}$ is ~4 times its value at 850 $\mathrm{m\,s^{-1}}$, but only 1.5 times it at 1000 $\mathrm{V\,cm^{-1}}$.

There are two contributing factors to the velocity dependence of the signals: ion-extraction efficiency and ionization distance. Both are dependent for a flat surface solely on the velocity component of the Rydberg atom along the surface normal. For the first factor, a larger extraction field is needed to pull the ion away from the surface for higher initial velocity [Eq. (3)]; the low-field onset of the ionization profile shifts to the right and thus the integrated signal decreases with increasing velocity. This variation with velocity is greater for ionization further from the surface (i.e., for the resonant case)—the second term in Eq. (3) becomes more important as D increases for a given value of T, thus F_{min} varies more with T (and hence with collisional velocity). Second, the more slowly moving atoms will have more time to be ionized at greater distances from the surface, even though the ionization rate is slow at such distances; hence, the mean ionization distance shifts to a larger value, reducing the minimum extraction field required, and the integrated signal decreases with velocity. Theoretical work for lower-n states [18] shows that the second effect is also more important for the resonant case. We believe the shape change happens because the resonance only occurs in a certain field range, and the velocity effects are likely to be different when the system is in the resonant field range compared to the off-resonant range. For the nonresonant case where ionization is at a shorter distance, the acceleration of the Rydberg atom as it gets closer to the surface (attracted by its own image charge) tends to dwarf the effects of varying the initial velocity. In this Letter we have demonstrated that the predicted resonances between hydrogen atom Rydberg states and the image states within the projected band gap of a Cu(100) surface are experimentally observable. The resonances occur in particular field ranges corresponding to a range of crossing between Rydberg and image states. Varying the velocity of the incoming beam provides a useful additional diagnostic for the existence of the resonance effects. This Letter shows that the Rydberg-surface collision experiment can lead to useful information about the electronic structure of the surface, not just the Rydberg atom itself. This type of experiment may be applicable to other systems where there is quantization of the surface states, e.g., for thin films or nanostructures, and such surfaces are currently under investigation. The attractiveness of using the Rydberg charge transfer arises from the wide range of energies that can be probed by populating different Rydberg quantum states.

[1] E. So, M. Dethlefsen, M. Ford, and T. P. Softley, Phys. Rev. Lett. **107**, 093201 (2011).

[2] E. So, M. T. Bell, and T. P. Softley, Phys. Rev. A **79**, 012901 (2009).

[3] J. Hanssen, C. F. Martin, and P. Nordlander, Surf. Sci. **423**, L271 (1999).
[4] F. B. Dunning, H. R. Dunham, C. Oubre, and P. Nordlander, Nucl. Instrum. Methods Phys. Res., Sect. B **203**, 69 (2003).
[5] G. E. McCown, C. R. Taylor, and C. A. Kocher, Phys. Rev. A **38**, 3918 (1988).
[6] G. Sashikesh, E. So, M. S. Ford, and T. P. Softley, Mol. Phys. **112**, 2495 (2014).
[7] R. P. Abel, C. Carr, U. Krohn, and C. S. Adams, Phys. Rev. A **84**, 023408 (2011).
[8] Y. Pu, D. D. Neufeld, and F. B. Dunning, Phys. Rev. A **81**, 042904 (2010).
[9] Y. Pu and F. B. Dunning, Phys. Rev. A **88**, 012901 (2013).
[10] E. Y. Usman, I. F. Urazgil'din, A. G. Borisov, and J. P. Gauyacq, Phys. Rev. B **64**, 205405 (2001).
[11] E. V. Chulkov, V. M. Silkin, and P. M. Echenique, Surf. Sci. **391**, L1217 (1997).
[12] U. Höfer, I. L. Shumay, C. Reu, U. Thomann, W. Wallauer, and T. Fauster, Science **277**, 1480 (1997).
[13] P. Wahl, M. A. Schneider, L. Diekhöner, R. Vogelgesang, and K. Kern, Phys. Rev. Lett **91**, 106802 (2003).
[14] D. Straub and F. J. Himpsel, Phys. Rev. B **33**, 2256 (1986).
[15] A. G. Borisov, A. K. Kazansky, and J. P. Gauyacq, Phys. Rev. Lett. **80**, 1996 (1998).
[16] A. G. Borisov, J. P. Gauyacq, A. K. Kazansky, E. V. Chulkov, V. M. Silkin, and P. M. Echenique, Phys. Rev. Lett. **86**, 488 (2001).
[17] T. Hecht, H. Winter, A. G. Borisov, J. P. Gauyacq, and A. K. Kazansky, Phys. Rev. Lett. **84**, 2517 (2000).
[18] E. So, J. A. Gibbard, and T. P. Softley, J. Phys. B **48**, 175205 (2015).
[19] D. Baye, Phys. Status Solidi B **243**, 1095 (2006).
[20] S. Willitsch, J. M. Dyke, and F. Merkt, Helv. Chim. Acta **86**, 1152 (2003).
[21] C. Seiler, S. D. Hogan, H. Schmutz, J. A. Agner, and F. Merkt, Phys. Rev. Lett. **106**, 073003 (2011).
[22] D. D. Neufeld, H. R. Dunham, S. Wethekam, J. C. Lancaster, and F. B. Dunning, Phys. Rev. B **78**, 115423 (2008).